

RUSSOITE, $\text{NH}_4\text{ClAs}^{3+}_2\text{O}_3(\text{H}_2\text{O})_{0.5}$, A NEW PHYLLOARSENITE MINERAL FROM SOLFATARA DI POZZUOLI, NAPOLI, ITALY

ITALO CAMPOSTRINI, FRANCESCO DEMARTIN, AND MARCO SCAVINI

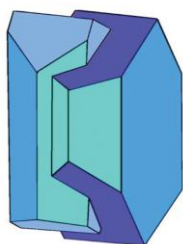
Università degli Studi di Milano, Dipartimento di Chimica, via Golgi 19, I-20133 Milano, Italy.

E-mail: francesco.demartin@unimi.it

[Received 8 August 2017; Accepted 23 November 2017; Associate Editor: Charles Geiger]

ABSTRACT

The new mineral russoite (IMA 2015-105), $\text{NH}_4\text{ClAs}^{3+}_2\text{O}_3(\text{H}_2\text{O})_{0.5}$, was found at the Solfatara di Pozzuoli, Pozzuoli, Napoli, Italy, as a fumarolic phase associated with alacranite, dimorphite, realgar, mascagnite, salammoniac and an amorphous arsenic sulfide. It occurs as hexagonal plates up to about 300 μm in diameter and 15 μm thick, in rosette-like intergrowths. On the basis of PXRD measurements and chemical analysis, the mineral was recognized to be identical to the corresponding synthetic phase $\text{NH}_4\text{ClAs}_2\text{O}_3(\text{H}_2\text{O})_{0.5}$. Crystals are transparent and colorless, with vitreous lustre and white streak. Tenacity is brittle and fracture is irregular. Cleavage is perfect on {001}. The measured density is 2.89(1) g/cm^3 , the calculated density is 2.911 g/cm^3 . The empirical formula, (based on 4.5 anions *pfu*) is $[(\text{NH}_4)_{0.94}, \text{K}_{0.06}]_{\Sigma 1.00}(\text{Cl}_{0.91}, \text{Br}_{0.01})_{\Sigma 0.92}\text{As}_{2.02}\text{O}_3(\text{H}_2\text{O})_{0.5}$. Russoite is hexagonal, space group *P622*, with $a = 5.2411(7)$, $c = 12.5948(25)$ Å, $V = 299.62(8)$ Å³ and $Z = 2$. The eight strongest X-ray powder diffraction lines are [d_{obs} Å(*hkl*)]: 12.63(19)(001), 6.32(100)(002), 4.547(75)(100), 4.218(47)(003), 3.094(45)(103), 2.627(46)(110), 2.428(31)(112) and 1.820(28)(115). The structure, was refined to $R = 0.0518$ for 311 reflections with $I > 2\sigma(I)$ and shows a different location of the ammonium cation and water molecules with respect to that reported for the synthetic analogue. The



Mineralogical Society

This is a 'preproof' accepted article for Mineralogical Magazine. This version may be subject to change during the production process.

DOI: 10.1180/minmag.2017.081.097.

mineral belongs to a small group of phylloarsenite minerals (lucabindiite, torrecillasite, gajardoite). It contains electrically neutral As_2O_3 layers, topologically identical to those found in lucabindiite and gajardoite between which are ammonium cations and outside of which Cl^- anions. Water molecules and additional ammonium cations are located in a layer between two levels of chloride anions.

Keywords: russoite; new mineral; arsenite; lucabindiite; torrecillasite; gajardoite.

INTRODUCTION

The Solfatara di Pozzuoli is one of about 40 volcanoes in the Campi Flegrei area and is located three kilometers from the center of the town of Pozzuoli, Napoli, Italy. Solfatara formed during the third Flegrean eruptive period and dates to about 3700-3900 years ago. Inside the Solfatara some active fumaroles are present, the most important of which is called "Bocca Grande" and has a temperature of about 160 °C. During a research campaign carried out in 2011, a few samples of the new mineral russoite, $\text{NH}_4\text{ClAs}^{3+}_2\text{O}_3(\text{H}_2\text{O})_{0.5}$, were collected at the "Bocca Grande" fumarole, where this phase formed as a sublimate product. XRPD measurements and chemical analysis, showed the mineral to be identical to the corresponding synthetic phase $\text{NH}_4\text{ClAs}_2\text{O}_3(\text{H}_2\text{O})_{0.5}$ (Edstrand and Blomqvist, 1955). In lack of single crystal suitable for an accurate X-ray structure refinement on the natural product, the XRPD data and the analytical results, perfectly matching those of the synthetic phase, were considered to be sufficient for a positive identification of the new mineral species, which was approved by the IMA Commission on New Minerals, Nomenclature and Classification (IMA. 2015-105). Its name was chosen to honour Dr. Massimo Russo (b. 1960, –), researcher at Osservatorio Vesuviano, Istituto Nazionale di Geofisica e Vulcanologia, Napoli. His work has been mainly devoted to the mineralogy of Italian volcanoes and he is author of several books and articles on this topic. Holotype material is deposited in the Reference Collection of the DCSSI, Università degli Studi di Milano, catalogue number 2015-01.

The recent availability of new material allowed us to obtain more accurate single-crystal intensity data for structure refinement. These data showed a location of the ammonium cation and water molecule

different from that proposed by Edstrand and Blomqvist (1955).

OCCURRENCE, CHEMICAL DATA AND PHYSICAL PROPERTIES

The new mineral russoite was found as a fumarolic phase associated with alacranite, dimorphite, mascagnite, realgar, salammoniac and an amorphous arsenic sulfide. In the same fumarole other interesting and rare minerals are found: adranosite, adranosite-(Fe), efremovite, huizingite-(Al) and godovikovite. Russoite occurs as rosette-like intergrowths or subparallel aggregates formed by hexagonal plates flattened on {001} and bounded by {100} up to about 300 μm in diameter and 15 μm thick, (Figures 1-2). These aggregates sometimes are yellowish due to admixed amorphous arsenic sulfide. Crystals are colorless to white, transparent or translucent, with vitreous lustre and white streak. Tenacity is brittle and fracture is irregular. Cleavage is perfect on {001}. The mineral does not fluoresce in long- or short-wave ultraviolet light. No twinning is apparent. The density, measured by flotation in a diiodomethane/benzene solution is 2.89(1) g/cm^3 , that calculated using the empirical formula and unit-cell data is 2.911 g/cm^3 . Due to the minute size of the crystals the Mohs hardness could not be determined. Optically russoite is uniaxial (-) with $\omega = 1.810(6)$ and $\varepsilon = 1.650(5)$ (measured in white light). The calculated mean refractive index using the Gladstone-Dale constants of Mandarino (1976, 1981) is 1.757, which is rated as good.

The infrared spectrum of russoite (Figure 3) was recorded in a KBr disk, in the range 4000 – 400 cm^{-1} , using a Jasco FTIR-470 Plus spectrometer. It is consistent with the presence of ammonium [bands at (cm^{-1}): 3254, ν_3 ; 3145, $2\nu_2$; 1403, ν_4], water [bands at (cm^{-1}): 3454, ν_3 ; 3398, ν_1 ; 1625, ν_2] and arsenite (bands at 604 and 670 cm^{-1}) (Farmer, 1974; Busigny et al., 2003). The weak absorption at about 2400 cm^{-1} is due to atmospheric CO_2 , that at 1110 cm^{-1} might be attributed to minor OH^- , partially replacing the chloride ion.

Quantitative chemical analyses (6) were carried out in EDS mode using a JEOL JSM 5500 LV scanning electron microscope equipped with an IXRF EDS 2000 microprobe (20 kV excitation voltage, 10 pA beam current, 2 μm beam diameter). This analytical method was chosen because crystal intergrowths did not take a good polish and was impossible to prepare a flat polished sample; moreover the crystals are severely damaged by using the WDS technique, even with a low voltage and current and a large diameter of the electron beam. In this case, as reported by Ruste (1979) and Acquafredda and Paglionico (2004), the EDS detector gives more accurate analyses of small volumes of investigated sample also with a probe current lower than 1 nA and this method gives good results also when collecting X-rays emitted from a non perfectly flat surface of the specimen. X-ray intensities were converted to wt% by ZAF quantitative analysis software. The standards employed were: synthetic InAs (As) halite (Cl), synthetic KBr (K, Br). Element concentrations were measured using the $K\alpha$ lines for Cl, K, and the $L\alpha$ line for As and Br. The mean analytical results are reported in Table 1. No amounts of other elements above 0.1 wt% were detected. Water and ammonium contents were not analyzed because the mineral is intimately mixed with mascagnite and realgar and is not possible to obtain a sufficient amount of pure sample suitable for this kind of analysis. The presence of N was also evident in the EDS spectrum made on selected crystals, however the uncertainties of the measurements were considered too large for a quantitative estimation of this element. Therefore the ammonium and water contents were deduced from the $\text{NH}_4\text{ClAs}_2\text{O}_3(\text{H}_2\text{O})_{0.5}$ stoichiometry, taking into account the K content, which partly replaces the ammonium ion ($\text{K} + \text{NH}_4 = 1$ apfu). The empirical formula (based on 4.5 anions *pfu*) is: $[(\text{NH}_4)_{0.94}, \text{K}_{0.06}]_{\Sigma 1.00}(\text{Cl}_{0.91}, \text{Br}_{0.01})_{\Sigma 0.92}\text{As}_{2.02}\text{O}_3(\text{H}_2\text{O})_{0.5}$. The simplified formula is $\text{NH}_4\text{ClAs}_2\text{O}_3(\text{H}_2\text{O})_{0.5}$.

The X-ray powder-diffraction pattern (Table 2), obtained using a conventional Rigaku DMAX II diffractometer, with graphite monochromatized $\text{CuK}\alpha$ radiation, is in good agreement with that calculated for the synthetic phase (PDF2 – entry 00-076-1366), whose structure was solved by Edstrand and Blomqvist (1955) on the basis of Weissenberg film measurements. Using the same indexing of the synthetic phase and the program UNITCELL (Holland and Redfern, 1997) the

following unit-cell parameters $a = 5.259(2)$, $c = 12.590(5)$ Å, $V = 301.55(2)$ Å³ were refined for russoite. They are in good agreement with those reported for the synthetic phase $a = 5.254$, $c = 12.574$ Å.

SINGLE-CRYSTAL STRUCTURE DETERMINATION

A new sampling, carried out in April 2016, after the approval of russoite as a new mineral by the IMA CNMNC, gave the us opportunity to collect additional specimens with larger aggregates of crystals (up to 0.3 mm), from which fragments apparently suitable for single-crystal structure determination could have been obtained. Indeed, all these fragments are not perfect single crystals, as they are made by several small platelets almost stacked in a parallel way, but slightly misaligned. After many attempts, one fragment was found to be composed by two different individuals only, sufficiently misaligned to allow the collection of a complete set of reflections, suitable for a new structure refinement. The diffracted intensities, corresponding to a complete scan of the reciprocal lattice up to $2\theta = 63.60^\circ$, were collected at room temperature using a Bruker Apex II diffractometer equipped with a 2K CCD detector and MoK α radiation ($\lambda = 0.71073$ Å). A one-minute frame-time and a 0.5° frame width were used. The intensity data were reduced using the program *SAINT* (Bruker, 2001), and corrected for Lorentz, polarization and background. An absorption correction ($\mu = 11.39$ mm⁻¹, $T_{\min} = 0.465$) was applied using the *SADABS* program (Sheldrick, 2000). Details about the data collection and refinement are summarized in Table 3.

Starting from the atomic coordinates reported by Edstrand and Blomqvist (1955) we refined the structure in the *P622* space group, using the *SHELXL97* program (Sheldrick, 2008) implemented in the *WinGX* suite (Farrugia, 1999). This refinement apparently confirmed the atomic positions found by these authors for all the atoms, with the only exception of the location of the ammonium ion on the *2d* Wyckoff position $[1/3, 2/3, 1/2]$. It should be noted that the ammonium position was chosen by Edstrand and Blomqvist between two possible residuals in the electron density map, since it was the

only one which assured reasonable ammonium-chloride distances, and the correct charge balance, if fully occupied. In our Difference-Fourier map we found instead no significant electron density at the $2d$ Wyckoff position, but an electron density residual of about $4.4 \text{ e}^-/\text{\AA}^3$ at the $3g$ Wyckoff position $[1/2, 0, 1/2]$, which was thought at first to be compatible with the possible presence of the ammonium ion at this site. With this assumption, because the multiplicity of the ammonium site is 3 and that of the chloride site is 2, the occupation of the ammonium ion should have been fixed to the value of $2/3$ to maintain the charge balance between the ammonium and the chloride ions. However, even with partial occupation of this site, the ammonium ions are too close one another at a distance of $2.6315(4) \text{ \AA}$, which is unrealistic. To obtain a correct set of interatomic contacts among the ammonium ions, the occupancy of the site should have been $1/3$ only, but this does not fulfill charge balance. At this point we began to doubt that other atoms of the model proposed by Edstrand and Blomqvist were correctly assigned, even if they apparently refined correctly, in particular the location of the water molecules between two As_2O_3 layers. Our doubts have been supported also by the evidence that the large cations are located between the As_2O_3 layers in the structure of the other phylloarsenites (see later). Therefore we replaced the water molecule at the $1a$ Wyckoff position by an ammonium ion, and we considered the $3g$ Wyckoff position to be $1/3$ occupied by an additional ammonium and $1/3$ occupied by a water molecule. This model is confirmed by the values of the refined occupancies (see Table 4) of the site and by the correct interatomic contacts between symmetry-related and hydrogen-bonded ammonium cations and water molecules. Replacement of ammonium with minor potassium, as suggested by the chemical analysis, was also taken into account. The value of the refined occupancy of the N(1) site is in good agreement with the K content obtained from the chemical analysis. The H atoms of the water molecule and of the ammonium ion at $3g$ could not be located in a difference Fourier map, where residual peaks around O and N indicate a situation of disorder. The same happens for the hydrogen atoms of the ammonium N(1), which is located inside a regular hexagonal prismatic cavity, because the site symmetry is higher than the symmetry of the ammonium ion and each hydrogen is therefore distributed over a number of symmetry-related sites. The final R index is 0.0518 for 311 independent

data having $I > 2\sigma(I)$ and 21 parameters. The *MISSIM* algorithm in the *PLATON* program (Spek, 2003) suggests a possible *P6/mmm* (pseudo) symmetry for the non disordered atoms of the structure. The statistical test ($|E^2 - 1| = 0.876$) does not indicate unequivocally the centrosymmetric/non-centrosymmetric nature of russoite (expected value of 0.968 centrosymmetric, 0.736 non-centrosymmetric). Since the refinement in the space group *P6/mmm* gives a significantly higher final $R = 0.0606$ for 232 independent data with $I > 2\sigma(I)$, the correct space group for russoite seems to be *P622*. Fractional atomic coordinates, occupancies, and anisotropic displacement parameters are presented in Table 4. Selected interatomic distances are reported in Table 5.

CRYSTAL STRUCTURE OF RUSSOITE

The mineral, together with lucabindiite $(K, NH_4)As_4O_6(Cl, Br)$ (Garavelli et al., 2013), torrecillasite $Na(As, Sb)^{3+}_4O_6Cl$ (Kampf et al., 2014) and gajardoite $KCa_{0.5}As^{3+}_4O_6Cl_2 \cdot 5H_2O$ (Kampf et al., 2016), forms a small group of phylloarsenite minerals. All these phases contain electrically neutral As_2O_3 sheets consisting of $As^{3+}O_3$ pyramids that share O atoms to form six-membered rings. The large cations are located between the sheets and the halide anions are outside them.

Russoite has closer structural relationships with lucabindiite, $(K, NH_4)As_4O_6(Cl, Br)$ ($a = 5.2386(7)$, $c = 9.014(2)$ Å), a complex arsenite chloride found for the first time at La Fossa crater, Vulcano Island, Sicily, and with gajardoite $KCa_{0.5}As^{3+}_4O_6Cl_2 \cdot 5H_2O$ ($a = 5.2558(8)$, $c = 16.9666(18)$ Å). These minerals display similarity in their hexagonal unit-cell parameter a , whereas the c parameter is variable due to the different stacking sequence of the large cations, chloride ions and H_2O molecules. In russoite, lucabindiite and gajardoite, the conformation of the As_2O_3 layers (Figure 5a) is the same, with all the As apices, and therefore the stereoactive lone pair of each As^{3+} atom, pointing in the same direction normal to the layer (planar layers). In the orthorhombic torrecillasite (Figure 5b) one of the As apices points instead in the opposite direction (wavy layers). Planar As_2O_3 layers with interlayer regions containing M large cations, alternating with interlayer regions

containing halogen anions, are also present in a group of synthetic compounds isostructural with lucabindiite, studied by Pertlik (1988), having general formula MAs_4O_6X ($M = K, NH_4$; $X = Cl, Br, I$).

The peculiarity of russoite is that we have, in the region between two levels of chloride ions, a disordered layer of water molecules and ammonium cations, interacting each other via hydrogen bonds. The bond-valence analysis (Table 6) shows reasonable values with only one striking anomaly: the bond-valence sums for the Cl site is only 0.16 vu. Low values of the bond-valence sums for the Cl site have also been observed in lucabindiite (0.31 vu), torrecillasite (0.49 vu) and gajardoite (0.24 vu) and were interpreted by other authors (Kampf et al., 2016) to be possibly related to the strong repulsive effect of the As^{3+} lone pair, which is directed towards the Cl sites. The coordination of the As atoms is therefore characterized by the presence of three short As-O distances (1.7995(9) Å and three As...Cl longer interactions (3.3422(7) Å).

ACKNOWLEDGEMENTS

The authors are most indebted to Silvia Bruni for the FTIR measurements. Valuable suggestions and constructing comments for improving the manuscript have been given by Luca Bindi, Charles Geiger, Anthony Kampf and Peter Leverett.

REFERENCES

- Acquafredda, P. and Paglionico, A. (2004) SEM-EDS microanalyses of micro-phenocrysts of Mediterranean obsidians: a preliminary approach to source discrimination. *European Journal of Mineralogy*, **16**, 419–429.
- Brese, N.E. and O’Keeffe, M. (1991) Bond-valence parameters for solids. *Acta Crystallographica*, **B47**, 192–197.
- Brown, I.D. (2009) Recent developments in the methods and applications of the bond valence model. *Chemical Reviews*, **109**, 6858–6919.

- Brown, I.D. and Altermatt, D. (1985) Bond-valence parameters from a systematic analysis of the inorganic crystal structure database. *Acta Crystallographica*, **B41**, 244–247.
- Bruker (2001) SAINT, Bruker AXS Inc., Madison, Wisconsin.
- Busigny, V., Cartigny, P., Philippot, P. and Javoy, M. (2003) Ammonium quantification in muscovite by infrared spectroscopy. *Chemical Geology*, **198**, 21–31.
- Edstrand, M. and Blomqvist, G. (1955) The crystal structure of $\text{NH}_4\text{Cl}\cdot\text{As}_2\text{O}_3\cdot\frac{1}{2}\text{H}_2\text{O}$. *Arkiv för Kemi*, **8**, 245–256.
- Farmer, V.C. (1974) The Infrared Spectra of Minerals. *Mineralogical Society Monograph 4*. London, UK.
- Farrugia, L.J. (1999) WinGX suite for small-molecule single-crystal crystallography. *Journal of Applied Crystallography*, **32**, 837–838.
- Fischer, R.X. and Tillmanns, E. (1988) The equivalent isotropic displacement factor. *Acta Crystallographica*, **C44**, 775–776.
- Garavelli, A., Mitolo, D., Pinto, D. and Vurro, F. (2013) Lucabindiite, $(\text{K},\text{NH}_4)\text{As}_4\text{O}_6(\text{Cl},\text{Br})$, a new fumarole mineral from the "La Fossa" crater at Vulcano, Aeolian Islands, Italy. *American Mineralogist*, **98**, 470–477.
- Holland, T.J.B. and Redfern, S.A.T. (1997) Unit cell refinement from powder diffraction data: the use of regression diagnostics. *Mineralogical Magazine*, **61**, 65–77.
- Kampf, A.R., Nash, B.P., Dini, M. and Molina Donoso, A.A. (2014) Torrecillasite, $\text{Na}(\text{As},\text{Sb})^3+_4\text{O}_6\text{Cl}$, a new mineral from the Torrecillas mine, Iquique Province, Chile: description and crystal structure. *Mineralogical Magazine*, **78**, 747–755.
- Kampf, A.R., Nash, B.P., Dini, M. and Molina Donoso, A.A. (2016) Gajardoite, $\text{KCa}_{0.5}\text{As}^3+_4\text{O}_6\text{Cl}_2\cdot 5\text{H}_2\text{O}$, a new mineral related to lucabindiite and torrecillasite from the Torrecillas mine, Iquique Province, Chile. *Mineralogical Magazine*, **80**, 1265–1272.
- Mandarino, J. A. (1976) The Gladstone-Dale relationship I. Derivation of new constants. *The Canadian Mineralogist*, **14**, 498–502.

- Mandarino, J.A. (1981) The Gladstone-Dale relationship. IV. The compatibility index and its application. *The Canadian Mineralogist*, **19**, 441–450.
- Pertlik, F. (1988) $\text{KAs}_4\text{O}_6\text{X}$ ($\text{X} = \text{Cl, Br, I}$) and $\text{NH}_4\text{As}_4\text{O}_6\text{X}$ ($\text{X} = \text{Br, I}$): hydrothermal syntheses and structure determinations. *Monatshefte für Chemie*, **119**, 451–456.
- Ruste, J. (1979) X-ray spectrometry. In Maurice, F., Meny, L., and Tixier, R., Eds., *Microanalysis and Scanning Electron Microscopy, Summer School St-Martin-d'Hères, France, September 11–16 (1978)*, 215–267. Les Editions de Physique, Orsay.
- Sheldrick, G.M. (2000) *SADABS Area-Detector Absorption Correction Program*, Bruker AXS Inc., Madison, WI, USA.
- Sheldrick, G.M. (2008) A short history of SHELX. *Acta Crystallographica*, **A64**, 112–122.
- Spek, A.L. (2003) Single-crystal structure validation with the program PLATON. *Journal of Applied Crystallography*, **36**, 7–13.

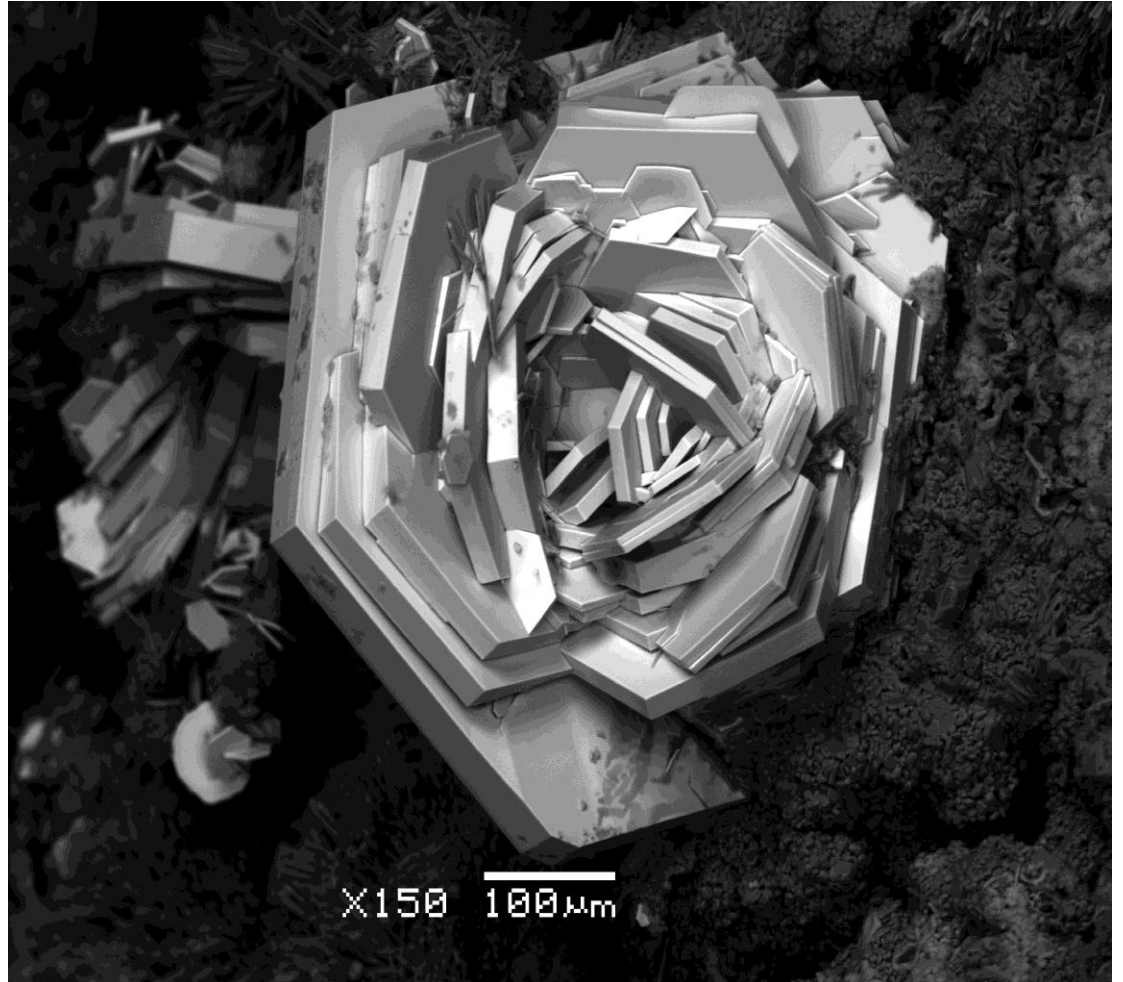


Figure 1. SEM-BSE image of rosette-like aggregates of russoite.

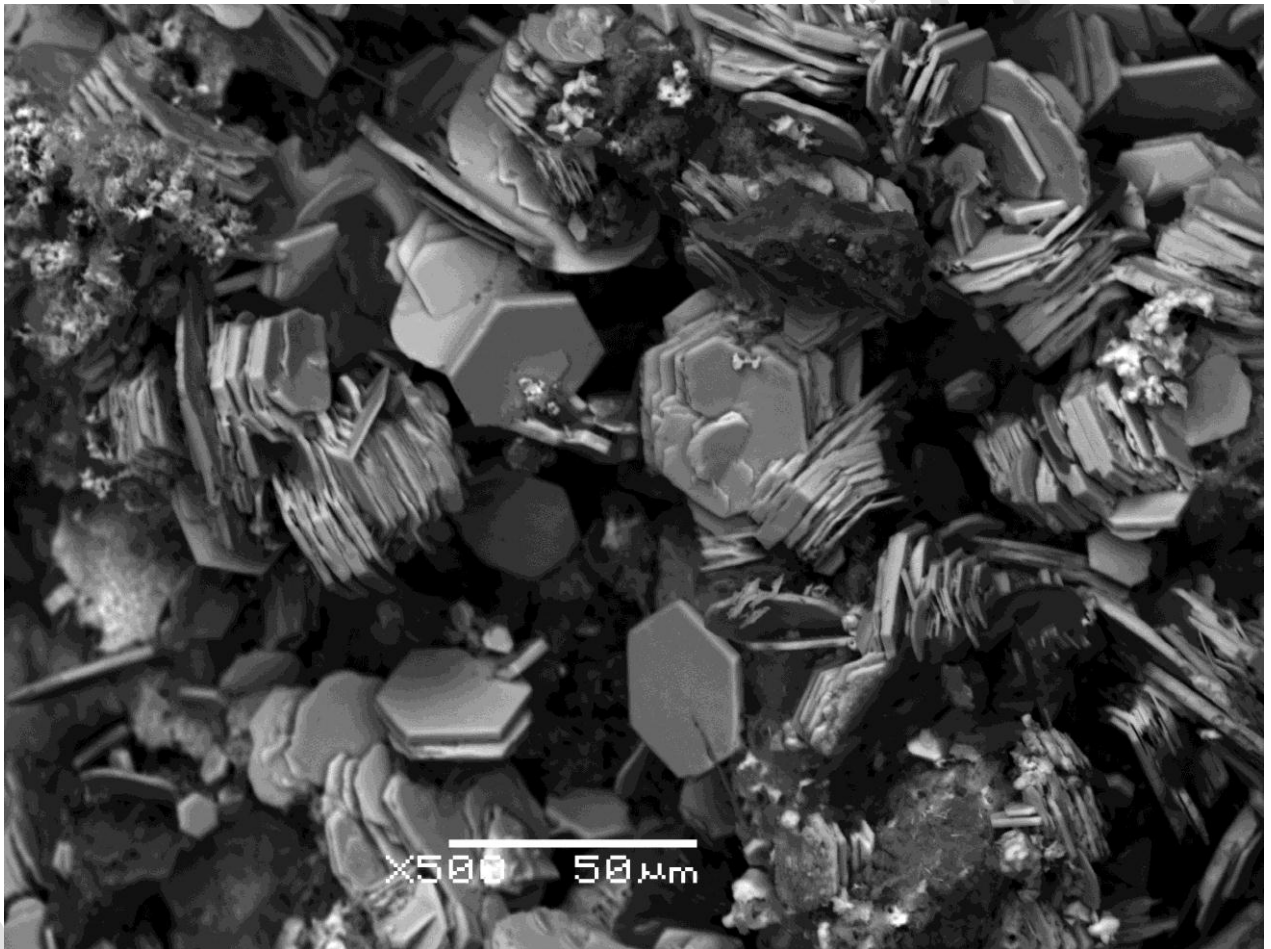


Figure 2. SEM-BSE image of subparallel crystal aggregates of russoite.

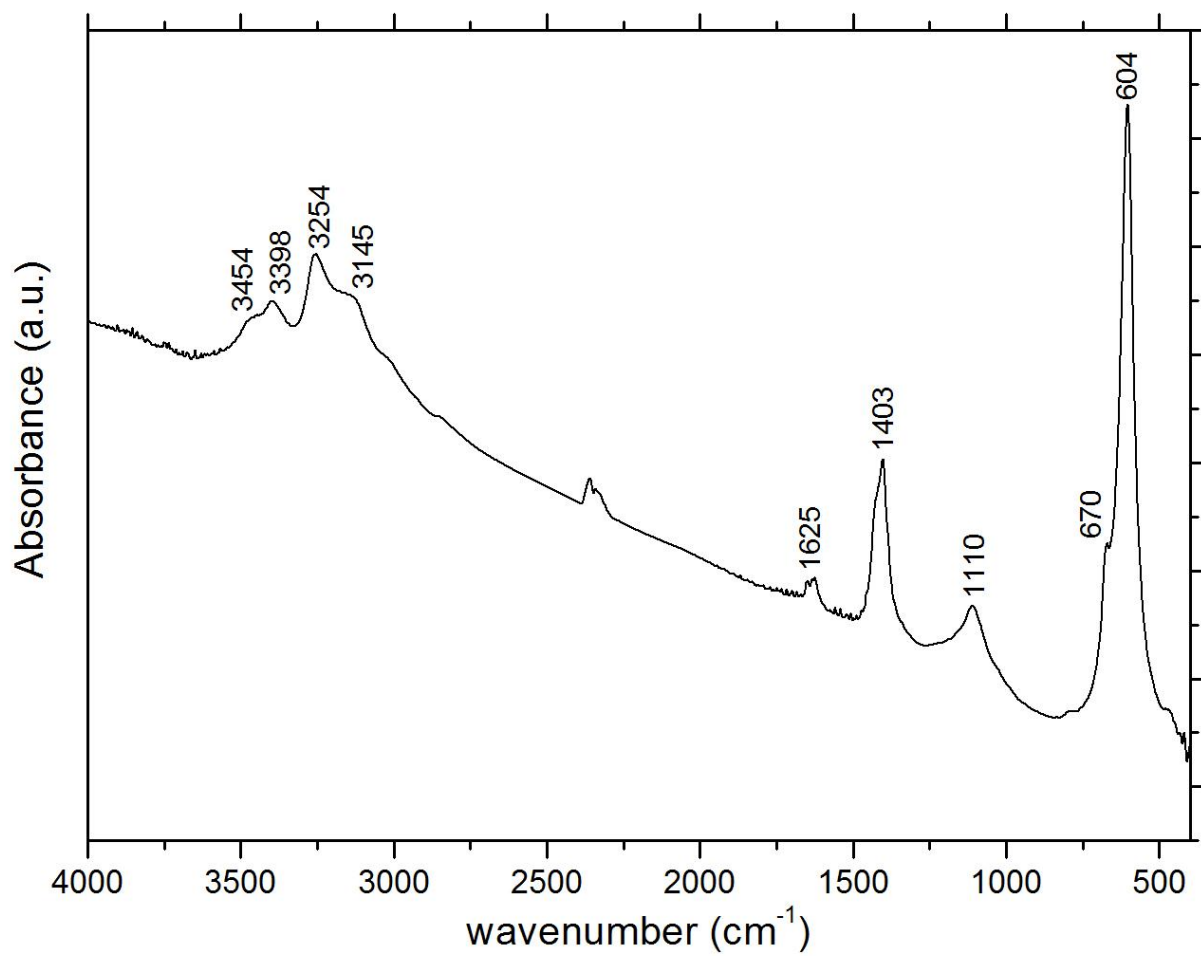


Figure 3. FT-IR spectrum of russoite

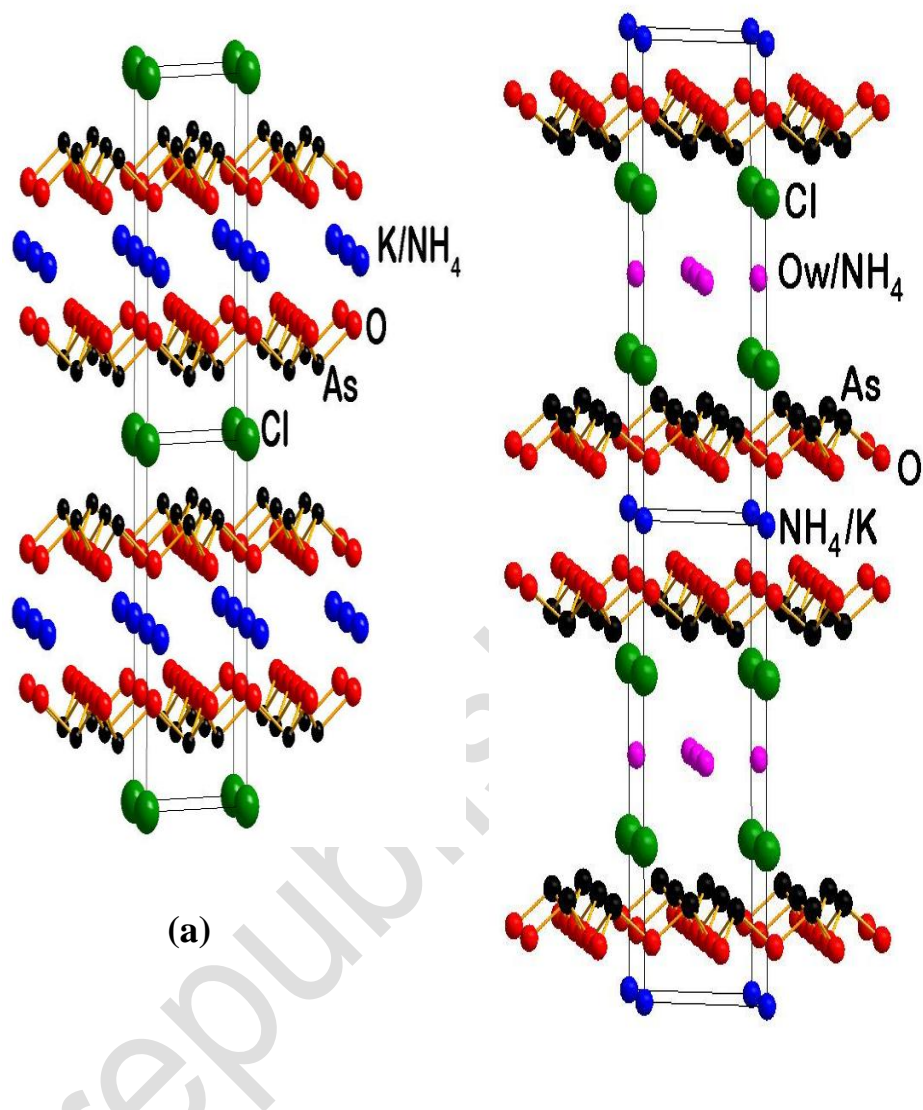
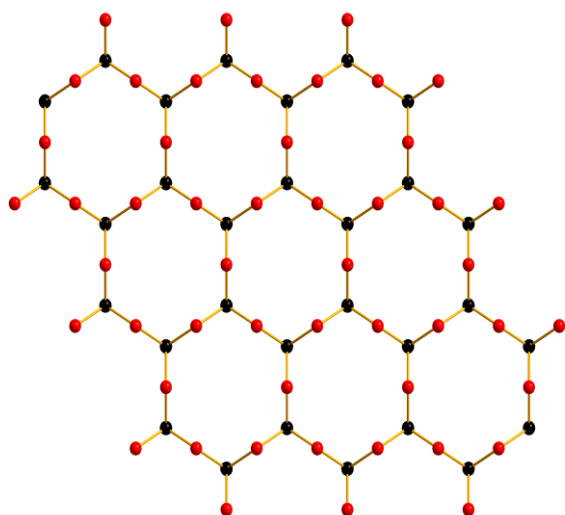
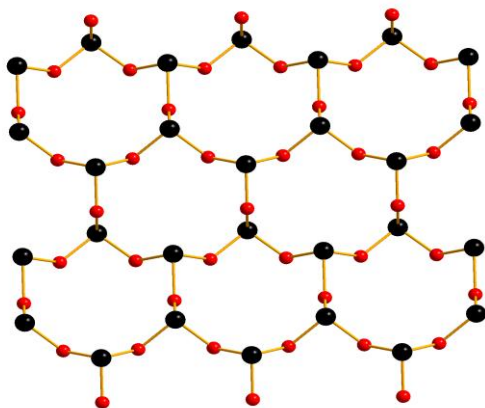


Figure 4. A comparison between the structure of lucabindiite (a) and that of russoite (b).



(a)



(b)

Figure 5. As_2O_3 sheets in russoite, lucabindiite, gajardoite (a) and torrecillasite (b); As black spheres, O red spheres.

Table 1. Analytical data for russoite (average of 6 analyses).

Constituent	Mean	Range	Stand. Dev.	Probe Standard
As ₂ O ₃	74.16	73.25-75.80	0.65	synthetic InAs
Cl	11.96	11.73-12.94	0.44	halite
Br	0.44	0.25-0.80	0.31	synthetic KBr
K ₂ O	1.05	0.65-1.22	0.12	synthetic KBr
(NH ₄) ₂ O*	9.04	-		
H ₂ O*	3.35	-		
	100.00			
-O=Cl, Br	-2.75			
Total	97.25			

* calculated by stoichiometry

The empirical formula (based on 4.5 anions *pfu*) is:

$[(\text{NH}_4)_{0.94}, \text{K}_{0.06}]_{\Sigma 1.00}(\text{Cl}_{0.91}, \text{Br}_{0.01})_{\Sigma 0.92} \text{As}_{2.02} \text{O}_3 (\text{H}_2\text{O})_{0.5}$.

The simplified formula is $\text{NH}_4\text{ClAs}_2\text{O}_3(\text{H}_2\text{O})_{0.5}$.

Table 2. X-ray powder-diffraction data for russoite and a comparison with the $\text{NH}_4\text{ClAs}_2\text{O}_3(\text{H}_2\text{O})_{0.5}$ synthetic analogue (PDF2 – entry 00-076-1366).

russoite				PDF2 00-076-1366 [§]		
I_{calc}^{**}	I/I_0	$d_{\text{obs}}(\text{Å})$	$d_{\text{calc}}(\text{Å})^*$	$d(\text{Å})$	I/I_0	$h\ k\ l$
58	19	12.63	12.590	12.574	63	0 0 1
100	100	6.32	6.295	6.287	100	0 0 2
22	75	4.547	4.554	4.550	18	1 0 0
18	8	4.283	4.283	4.279	10	1 0 1
23	47	4.218	4.197	4.191	21	0 0 3
20	11	3.695	3.690	3.686	15	1 0 2
57	45	3.094	3.086	3.083	55	1 0 3
50	46	2.627	2.629	2.627	42	1 1 0
2	13	2.522	2.518	2.515	2	0 0 5
55	31	2.428	2.427	2.424	29	1 1 2
1	12	2.273	2.278	2.275	1	2 0 0
4	4	2.229	2.229	2.226	4	1 1 3
12	10	2.211	2.204	2.201	6	1 0 5
1	4	2.096	2.098	2.096	1	0 0 6
10	8	2.021	2.018	2.016	10	1 1 4
1	4	1.902	1.906	1.904	1	1 0 6
6	4	1.847	1.845	1.843	5	2 0 4
12	28	1.820	1.819	1.817	7	1 1 5
3	6	1.794	1.799	1.796	1	0 0 7
2	4	1.718	1.722	1.720	2	2 1 0
1	7	1.706	1.706	1.704	1	2 1 1
2	4	1.671	1.673	1.671	2	1 0 7
4	5	1.594	1.593	1.591	6	2 1 3
1	5	1.574	1.574	1.572	1	0 0 8

[§] Pattern calculated from ICSD using POWD-12++

* Calculated from the unit cell ($a = 5.259(2)$ Å; $c = 12.590(5)$ Å) obtained from least-squares refinement from the above data using the program UNITCELL (Holland and Redfern, 1997).

** Calculated from our structure data.

Table 3. Single-crystal diffraction data and refinement parameters for russoite

Crystal system	hexagonal
Space Group	<i>P</i> 622 (no. 177)
<i>a</i> (Å)	5.2411(7)
<i>c</i> (Å)	12.5948(25)
<i>V</i> (Å ³)	299.62(8)
<i>Z</i>	2
Radiation	MoK α
μ (mm ⁻¹)	11.39
D _{calc} (g cm ⁻³)	2.911
Reflections measured	3196
Independent reflections	354
Observed reflections [<i>I</i> > 2 σ (<i>I</i>)]	311
Parameters refined	21
Final <i>R</i> [<i>I</i> > 2 σ (<i>I</i>)] and w <i>R</i> 2 (all data)	0.0518, 0.1010
Goof	1.211

Notes: $R = \frac{\sum ||F_o| - |F_c||}{\sum |F_o|}$; $wR2 = \left\{ \frac{\sum [w(F_o^2 - F_c^2)^2]}{\sum [w(F_o^2)^2]} \right\}^{1/2}$;

$w = 1 / [\sigma^2(F_o^2) + (0.0625q)^2]$ where $q = [\max(0, F_o^2) + 2F_c^2] / 3$;

Goof = $\left\{ \frac{\sum [w(F_o^2 - F_c^2)]}{(n-p)} \right\}^{1/2}$ where *n* is the number of reflections and *p* is the number of refined parameters.

Table 4. Atomic coordinates and displacement parameters [$U_{eq}/U(i,j)$, Å²] for russoite

Atom	Wyckoff letter	occupancy	x/a	y/b	z/c	U_{eq}
As	4 <i>h</i>	1	1/3	2/3	0.21224(2)	0.01708(6)
O	6 <i>i</i>	1	0	1/2	0.13607(13)	0.0202(4)
Cl	2 <i>e</i>	1	0	0	0.32220(10)	0.0340(2)
N(1)	1 <i>a</i>	0.936(6)	0	0	0	0.0323(11)
K(1)	1 <i>a</i>	0.064(6)	0	0	0	0.0323(11)
N(2)	3 <i>g</i>	0.341(12)	1/2	0	1/2	0.098(3)
Ow	3 <i>g</i>	0.340(10)	1/2	0	1/2	0.098(3)

Atom	U_{11}	U_{22}	U_{33}	U_{23}	U_{13}	U_{12}
As	0.01357(7)	0.01357(7)	0.02411(13)	0	0	0.0678(3)
O	0.0121(5)	0.0168(4)	0.0281(7)	0	0	0.0046(5)
Cl	0.0313(3)	0.0313(3)	0.0395(5)	0	0	0.0156(1)
N(1)/K(1)	0.0277(11)	0.0277(11)	0.041(2)	0	0	0.0138(6)
N(2)/Ow	0.145(7)	0.067(5)	0.057(4)	0	0	0.33(2)

The anisotropic displacement factor exponent takes the form:

$$-2\pi^2(U_{11}h^2(a^*)^2 + \dots + 2U_{12}hka^*b^* + \dots); U_{eq} \text{ according to Fischer and Tillmanns (1988).}$$

Table 5. Selected interatomic distances (Å) and angles (deg.) in russoite

As-O (×3)	1.7995(9)	Cl [−] ⋯O (×6)	3.532(1)
As ³⁺ ⋯Cl (×3)	3.3422(7)	N(2) ⁺ ⋯Ow	2.6315(4)
As ³⁺ ⋯As (×3)	3.0386(4)		
Ow/N(2) ⁺ ⋯Cl (×4)	3.4628(9)	O-As-O (×3)	93.97(6)
N(1) ⁺ ⋯O (×12)	3.145(1)	As-O-As	115.19(9)
N(1) ⁺ ⋯Cl (×2)	4.079(1)		

Table 6. Bond-valence analysis for russoite (non disordered atoms). Values are expressed in valence units (vu).

	O	Cl	Σ_c
As	0.97 ×3→ 0.97 ×2↓	0.04 ×3	3.15
N(1)H ₄ ⁺	0.08 ×12→ 0.08 ×1↓	0.02 ×2→ 0.02×2↓	1.00
Σ_a	2.05	0.16	

As³⁺-O, As³⁺-Cl and NH₄⁺-Cl bond-valence parameters from Brown and Altermatt (1985), Brese and O'Keeffe (1991) and Brown (2009), respectively.